

A MATHEMATICAL HISTORY OF TAFFY PULLERS

JEAN-LUC THIFFEAULT

ABSTRACT. We describe a number of devices for pulling candy, called taffy pullers, that are related to pseudo-Anosov mapping classes. Though the mathematical connection has long been known for the two most common taffy puller designs, we unearth a rich variety of early designs from the patent literature.

1. INTRODUCTION

Taffy is a type of candy made by first heating sugar to a critical temperature, letting the mixture cool on a slab, then repeatedly ‘pulling’ — stretching and folding — the resulting mass. The purpose of pulling is to get air bubbles into the taffy, which gives it a nicer texture. Until the late 19th century, taffy was pulled by hand — an arduous task. The process was ripe for mechanization.

In the first decades of the 20th century there was a flurry of patents for taffy pullers, with many displaying innovative ideas. These were designed to repeatedly stretch and fold the taffy in a manner that would lead to exponential growth. What concerns us most here is their mathematical underpinning: we will show that the computation of the growth of the taffy leads to several interesting algebraic numbers, associated with the dilatation of pseudo-Anosov maps. The taffy pullers can be thought as concrete realizations of these maps, and so for a mathematician they provide convenient examples. It is also intriguing to ask which dilatations were ‘discovered’ by inventors of taffy pullers. For example, a practical device realizing the Golden Ratio as a dilatation is challenging to construct, but as we shall see was introduced as early as 1918.

Another reason for exploring these devices is that their design may hold lessons for improving modern mixers. In particular, the pharmaceutical industry often requires the mixing of delicate, expensive pastes that must be mixed in a manner very similar to the action of taffy pullers.

Acknowledgments. The author thanks Alex Flanagan for helping to design and build the 6-rod taffy puller.

Supported by NSF grant CMMI-1233935.

2. SOME HISTORY

The first patent for a mechanical taffy puller was by Firchau (1893). His design consisted of two counter-rotating rods on concentric circles, as depicted in Fig 1. A quick glance at the trajectories confirms that this is not a true taffy puller in the sense employed here: a piece of taffy wrapped around the rods will not grow exponentially. In the language of mapping classes, this rod motion is ‘finite-order’ (Farb and Margalit 2011; Fathi, Laudenbach, and Poénaru 1979; Thurston 1988). For us, taffy pullers must be pseudo-Anosov. Among other things, this means that the growth of taffy must be exponential, characterized by an algebraic integer called the dilatation. It also means that a piece of taffy must grow exponentially no matter which two rods it is initially laid across — no rod can be redundant. Perhaps surprisingly, essentially all the devices found in patents after Firchau give pseudo-Anosov mapping classes.

Firchau’s device would have been terrible at pulling taffy, but it was likely never built. In 1900, Herbert M. Dickinson invented the first mathematically interesting taffy puller, and described it in the trade journal *The Confectioner*. His machine, depicted in Fig. 2, involves a fixed rod and two reciprocating rods. The reciprocating rods are ‘tripped’ to exchange position when they reach the limit of their motion. Dickinson later patented the machine (Dickinson 1906) and assigned it to Herbert L. Hildreth, the owner of the Hotel Velvet on Old Orchard Beach, Maine. Taffy was especially popular at beach resorts, in the form of salt water taffy (which is not really made using salt water). Hildreth sold his ‘Hildreth’s Original and Only Velvet Candy’ to the Maine tourists as well as wholesale, so he needed to make large quantities of taffy. Though he was usually not the inventor, he was the assignee on several taffy-puller patents in the early 1900s. In fact several such patents were filed in a span of a few years by several inventors, which led to lengthy legal wranglings. Some of these legal issues were resolved by Hildreth buying out the other inventors; for instance, he acquired one such patent for \$75,000 (about two million of today’s dollars). Taffy was becoming big business.

Shockingly, the taffy patent wars went all the way to the US Supreme Court. The opinion of the Court was delivered by Chief Justice William Howard Taft. The opinion shows a keen grasp of topological dynamics (*Hildreth v. Mastoras*, 1921):

The machine shown in the Firchau patent [has two pins that] pass each other twice during each revolution [. . .] and move in concentric circles, but do not have the relative in-and-out motion or Figure 8 movement of the Dickinson machine. With only two hooks there could be no lapping of the candy, because there was no third pin to re-engage the candy while it was held between the other two pins.

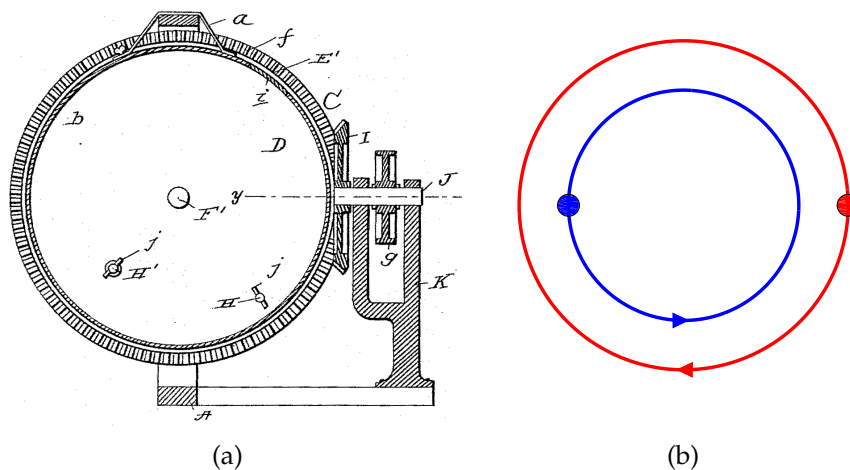


FIGURE 1. (a) Taffy puller from the patent of Firchau (1893), with two counter-rotating rods H and H' , fixed to separate disks. (b) The corresponding rod motion has no topological complexity.

The movement of the two pins in concentric circles might stretch it somewhat and stir it, but it would not pull it in the sense of the art.

The Supreme Court opinion displays the fundamental insight that at least three rods are required to produce some sort of rapid growth. Moreover, the ‘Figure 8’ motion is identified as key to this growth. We shall have more to say on this rod motion as we examine in turn the different design principles.

The Dickinson taffy puller in Fig. 2 is the earliest model that displays topological complexity. However, the design itself is overly complicated: it relies on a reciprocating mechanism, where two rods travel back and forth and are tripped by stops at each end, which causes them to exchange position. The net result is a rod motion as in Fig. 3(b). The reciprocating motion itself is difficult to achieve, relying on two straps coming from the same engine. It is doubtful that this device was ever used to make large quantities of candy. The vertical pins (as opposed to horizontal in all the other designs, with the candy hanging from them) suggest that the machine would be better used to stir candy, rather than pull it, as was pointed out by an expert witness in one of the lawsuits mentioned above.

The Dickinson device’s rod motion in Fig. 2(b) can be obtained by a much simpler mechanism, which was introduced in a patent by Robinson and Deiter (1908) and is still in use today. (Fig. 3). We call this design the *standard 3-rod taffy puller*. Comparing Figs. 2(b) and 3(b), we can see that the rod motion is identical

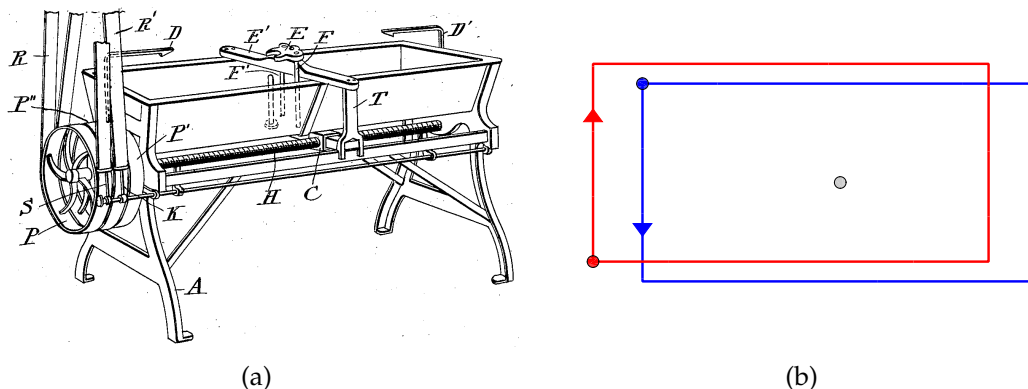


FIGURE 2. (a) Taffy puller from the patent of Dickinson (1906), with two reciprocating rods and a fixed rod. The reciprocating rods are tripped to exchange position when they reach the stops at D and D' . (b) The corresponding rod motion, with a fixed rod.

to the Dickinson design, up to deformation of the trajectories. In this puller the rods are horizontal, as they are for all pullers except Dickinson's.

3. TAFFY PULLERS WITH QUADRATIC DILATATION

As we shall see, there is a wide variety of designs for taffy pullers. There are a few more common ones, and in this section we will examine in detail the mathematics underpinning those where the 'growth constant' — the dilatation — is a quadratic number. Following a theorem of Franks and Rykken (1999), those can all be derived from Anosov maps of the torus.

3.1. Three-rod devices. Taffy pullers involving three rods (some of which may be fixed) are the easiest to describe mathematically. The action of arguably the simplest such puller, from the mathematical standpoint, is depicted in Fig. 4(a). By action, we mean the effect of the puller on a piece of abstract 'taffy.' For this puller the first and second rods are interchanged clockwise, then the second and third are interchanged counterclockwise. Here first, second, and third refer to the current *position* of a rod from left to right, not to the rod itself. Notice that each rod in Fig. 4(a) undergoes a 'Figure 8' motion.

Mathematically, we regard the taffy puller as a motion of three points in the plane, and we add the 'point at infinity' to get the Riemann sphere. Hence, we have three points moving on a two-dimensional sphere, and a fourth fixed point which does not correspond to a rod. The taffy is a loop on the sphere, winding around the points. We extend the action of the puller to the whole of the sphere,

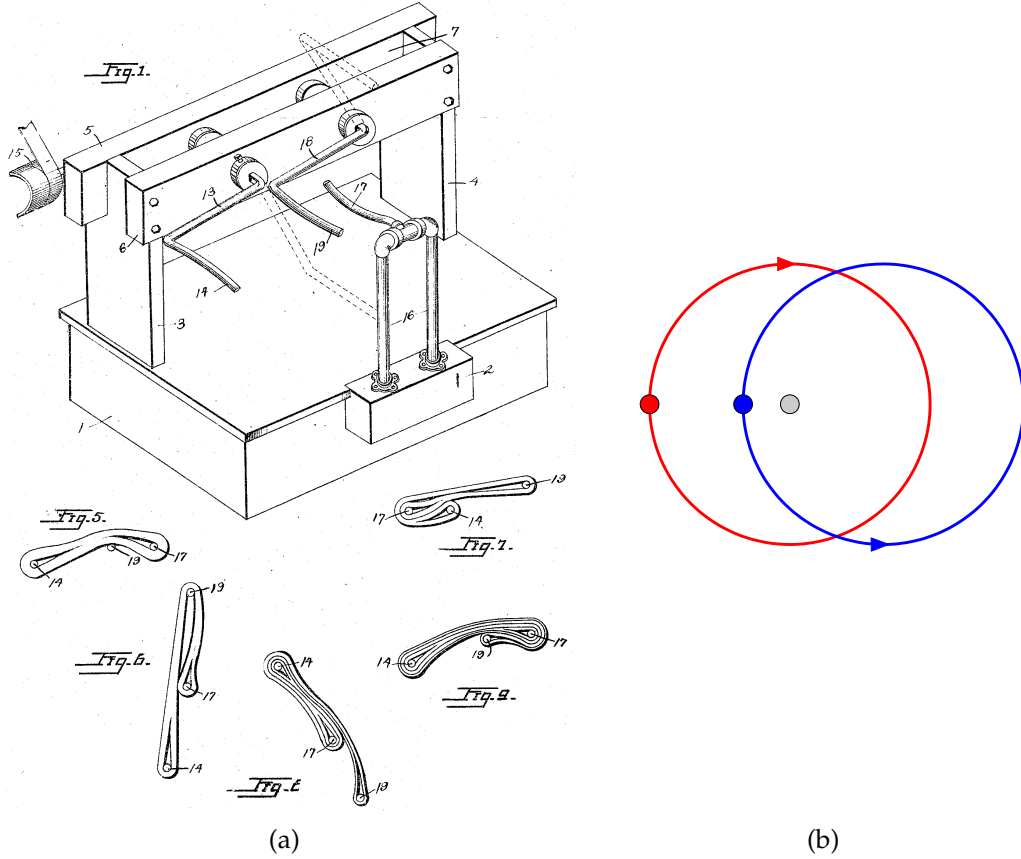


FIGURE 3. (a) Taffy puller from the patent of Robinson and Deiter (1908). (b) The motion of the rods.

so the taffy puller can be seen as a map of the sphere to itself. This map fixes one point, and fixes three other points as a set.

We now show that such maps arise naturally from linear maps on the torus (see for example Farb and Margalit (2011) for more details). Figure 5(a) shows the familiar two-dimensional torus, and Fig. 5(b) shows a model of the torus T^2 as the unit square $[0, 1]^2$ with opposite edges identified. Consider the linear map $\iota : T^2 \rightarrow T^2$, defined by $\iota(x) = -x \pmod{1}$. The map ι is an involution ($\iota^2 = \text{id}$) with four fixed points on the torus $[0, 1]^2$,

$$(1) \quad p_0 = \begin{pmatrix} 0 \\ 0 \end{pmatrix}, \quad p_1 = \begin{pmatrix} \frac{1}{2} \\ 0 \end{pmatrix}, \quad p_2 = \begin{pmatrix} \frac{1}{2} \\ \frac{1}{2} \end{pmatrix}, \quad p_3 = \begin{pmatrix} 0 \\ \frac{1}{2} \end{pmatrix},$$

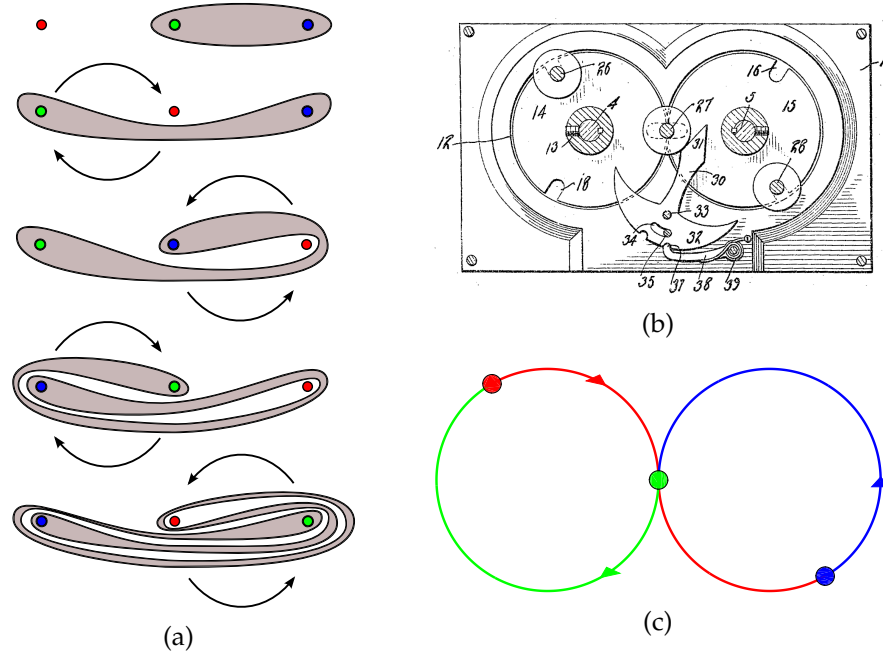


FIGURE 4. (a) The action of a 3-rod taffy puller. The first and second rods are interchanged clockwise, then the second and third rods are interchanged counterclockwise. Two periods are depicted. (b) Taffy puller from the patent of Nitz (1918). Rods alternate between the two wheels. (c) Each of the three rods moves in a Figure-8.

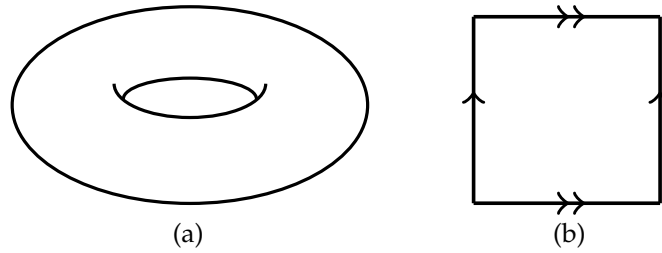


FIGURE 5. The torus (a) embedded in three dimensions and (b) as an unfolded surface with edge identifications.

since $-\frac{1}{2}$ is identified with $\frac{1}{2}$ after modding. Figure 6(a) shows how the different sections of T^2 are mapped to each other under ι ; arrows map to each other or are

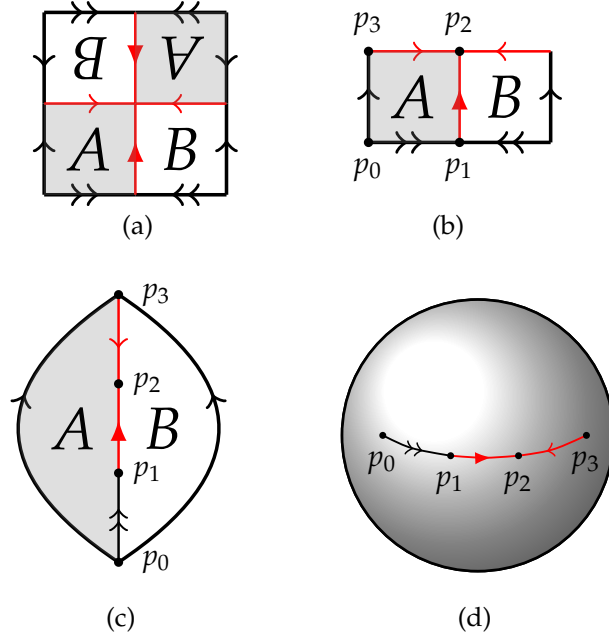


FIGURE 6. (a) Identification of regions on T^2 under the map ι . (b) The surface $S = T^2/\iota$, with the four fixed points of ι shown. (c) Partially zipped surface. (d) S is a sphere with four punctures, denoted $S_{0,4}$.

identified because of periodicity. Hence, the quotient space

$$(2) \quad S = T^2/\iota$$

can be depicted as in Fig. 6(b). The quotient space S is actually a sphere, in the topological sense (it has genus zero). We can see this by first ‘gluing’ or ‘zipping’ the identified edges at p_1 and p_2 to obtain Fig. 6(c). Then we zip between p_0 and p_3 , and we are left with a sphere as in Fig. 6(d). The sphere has 4 ‘punctures,’ so we write $S = S_{0,4}$, which indicates a surface of genus 0 with 4 punctures.

Now let’s take a linear map $\phi : T^2 \rightarrow T^2$ of the torus to itself. We write $\phi(x) = M \cdot x \bmod 1$, with $x \in [0, 1]^2$ and M a matrix in $SL_2(\mathbb{Z})$,

$$(3) \quad M = \begin{pmatrix} a & b \\ c & d \end{pmatrix}, \quad a, b, c, d \in \mathbb{Z}, \quad ad - bc = 1.$$

This guarantees that ϕ is an orientation-preserving homeomorphism. Obviously, the map $\phi(x)$ fixes $p_0 = (0 \ 0)^T$. Less obvious is that it *permutes* the ordered set (p_1, p_2, p_3) of points defined in (1). The image of each coordinate is some integer multiple of $\frac{1}{2}$, which after modding maps back to 0 or $\frac{1}{2}$. None of the points

can map to p_0 since it is a fixed point and ϕ is a homeomorphism. For example, the map

$$(4) \quad \phi(x) = \begin{pmatrix} 2 & 1 \\ 1 & 1 \end{pmatrix} \cdot x \mod 1$$

maps (p_1, p_2, p_3) to (p_3, p_1, p_2) . This is an *Anosov map*, since its trace has magnitude larger than 3, which means that it has a real eigenvalue larger than one (in magnitude). We call the spectral radius the *dilatation* of the map ϕ .

A linear map such as ϕ on the torus ‘descends’ or projects nicely to the punctured sphere $S_{0,4} = T^2/\iota$. We know this because all such linear maps commute with ι , since ι is just represented as the negative identity matrix. On $S_{0,4}$, the permuted fixed points (p_1, p_2, p_3) play the role of the rods of the taffy puller, and p_0 is the point at infinity. The induced map on $S_{0,4}$ is called *pseudo-Anosov* rather than Anosov, since the quotient of the torus by ι created four singularities.

Let’s show that the action of the map (4) gives the taffy puller in Fig. 4. Figure 7(a) (left) shows two curves on the torus, which project to curves on the punctured sphere $S_{0,4}$ (right). (We omit the sphere itself and just show the punctures.) Now if we act on the curves with the torus map (4), we obtain the curves in Fig. 7(b) (left). After taking the quotient with ι , the curves project down as in Fig. 7(b) (right). This has the same shape as our taffy in Fig. 4(a) (third frame), which corresponded to a period of the taffy puller. This suggests that the map (4) induces the same action on curves as the taffy puller, once we project from the torus to the punctured sphere $S_{0,4} = T^2/\iota$ using the involution ι .

What we’ve essentially shown is that the taffy puller in Fig. 4 can be described by an Anosov map. The growth of the length taffy, under repeated action, will be given by the largest eigenvalue λ of the matrix M , here $\lambda = \varphi^2$ with φ being the Golden Ratio $\frac{1}{2}(1 + \sqrt{5})$. This taffy puller is a bit peculiar in that it requires rods to move in a Figure-8 motion, as shown in Fig. 4(c). This is difficult to achieve mechanically, but surprisingly such a device was patented by Nitz (1918) (Fig. 4(b), and then apparently again by Kirsch (1928). The device requires rods to alternately jump between two rotating wheels.

All 3-rod devices can be treated in the same manner, including the standard 3-rod taffy puller depicted in Fig. 3. It arises from the linear map

$$(5) \quad \phi(x) = \begin{pmatrix} 5 & 2 \\ 2 & 1 \end{pmatrix} \cdot x \mod 1$$

which has $\lambda = \chi^2$. Here $\chi = 1 + \sqrt{2}$ is the *Silver Ratio* (Finn and Thiffeault 2011).

3.2. Four-rod devices. As discussed in the previous section, all 3-rod taffy pullers arise from Anosov maps of the torus. This is not true in general for more than

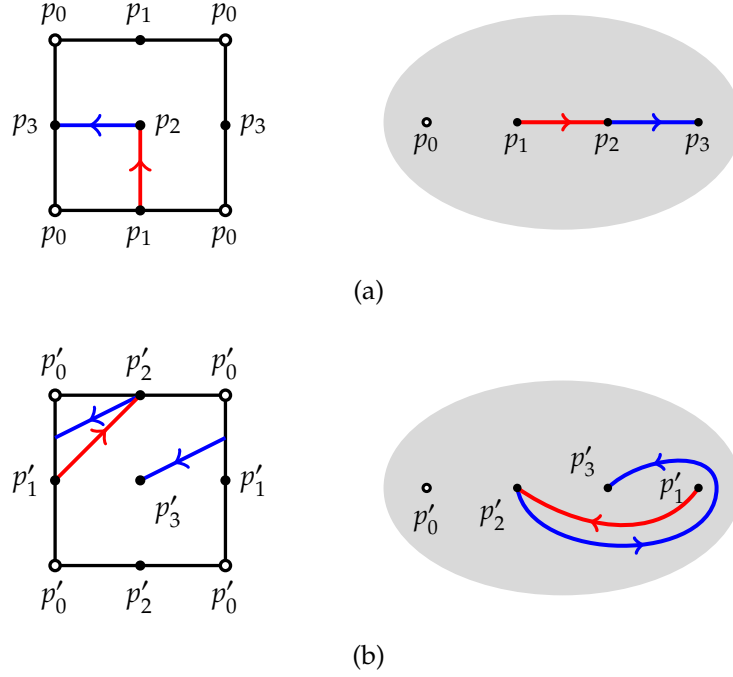


FIGURE 7. (a) Two curves on the torus T^2 (left), which project to curves on the punctured sphere $S_{0,4}$ (right). (b) The two curves transformed by the map (4) (left), and projected onto $S_{0,4}$ (right). The transformed blue curve is the same as in the third frame of Fig. 4(a).

three rods, but it is true for several specific devices. A theorem of Franks and Rykken (1999) states that if the dilatation λ of a pseudo-Anosov map is a quadratic number (i.e., satisfies $\lambda^2 - \tau\lambda + 1 = 0$ for some integer $\tau > 2$), then the map must come from a branched cover of the torus. We will investigate several examples in this and the next section.

Probably the most common device is the *standard 4-rod taffy puller*, which was invented by Thibodeau (1903) and is shown in Fig. 8. It seems to have been rediscovered several times, such as by Hudson (1904). The design of Richards (1905) is a variation that achieves the same effect, and his patent has some of the prettiest diagrams of taffy pulling in action (Fig. 9). Mathematically, the 4-rod puller was studied by MacKay (2001) and Halbert and Yorke (2014).

The rod motion for the standard 4-rod puller is shown in Fig. 8(b). Observe that the two orbits of smaller radius are not intertwined, so topologically they might as well be fixed rods. A full period of the puller requires that all the rods to return to their initial position. It may happen, though this is not always the case, that a taffy

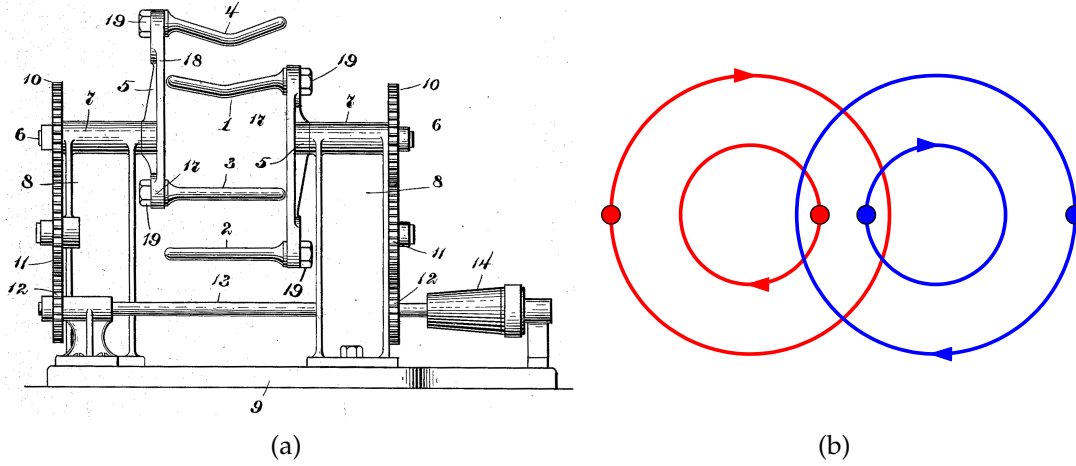


FIGURE 8. (a) Side view of the standard 4-rod taffy puller from the patent of Thibodeau (1903), with four rotating rods set on two axes. (b) Rod motion.

puller with 4 rods actually arises from an Anosov map such as (5), but with all four points (p_0, p_1, p_2, p_3) identified with rods, as opposed to one point being identified with the point at infinity in the 3-rod case. We relabel the four points (p_0, p_1, p_2, p_3) as $(1, 4, 3, 2)$, as in Fig. 10(a) (left), which gives the order of the rods on the right in that figure. (We shall discuss the point 0 below.)

Now act on the curves in Fig. 10(a) with the map

$$(6) \quad \phi(x) = \begin{pmatrix} 3 & 2 \\ 4 & 3 \end{pmatrix} \cdot x \pmod{1}.$$

This map fixes each of the points 1, 2, 3, 4, just as the 4-rod taffy puller does. Figure 10(b) shows the action of the map on curves anchored on the rods: it acts in exactly the same manner as the standard 4-rod taffy puller. In fact,

$$(7) \quad \begin{pmatrix} 3 & 2 \\ 4 & 3 \end{pmatrix} = \begin{pmatrix} 1 & 0 \\ 1 & 1 \end{pmatrix} \begin{pmatrix} 5 & 2 \\ 2 & 1 \end{pmatrix} \begin{pmatrix} 1 & 0 \\ 1 & 1 \end{pmatrix}^{-1}$$

which means that the maps (5) and (6) are *conjugate* to each other. Conjugate maps have the same dilatation (the trace is invariant), so the standard 3-rod and 4-rod taffy pullers arise from essentially the same Anosov map, only interpreted differently.

In the 3-rod case, a quotient of T^2 by the map ι gives $S_{0,4}$, a sphere with 4 punctures. In the 4-rod case, we need ι to give $S_{0,5}$ in order to have a ‘point at infinity.’ There are no more fixed points available, since $\phi(x)$ only has 4. However,

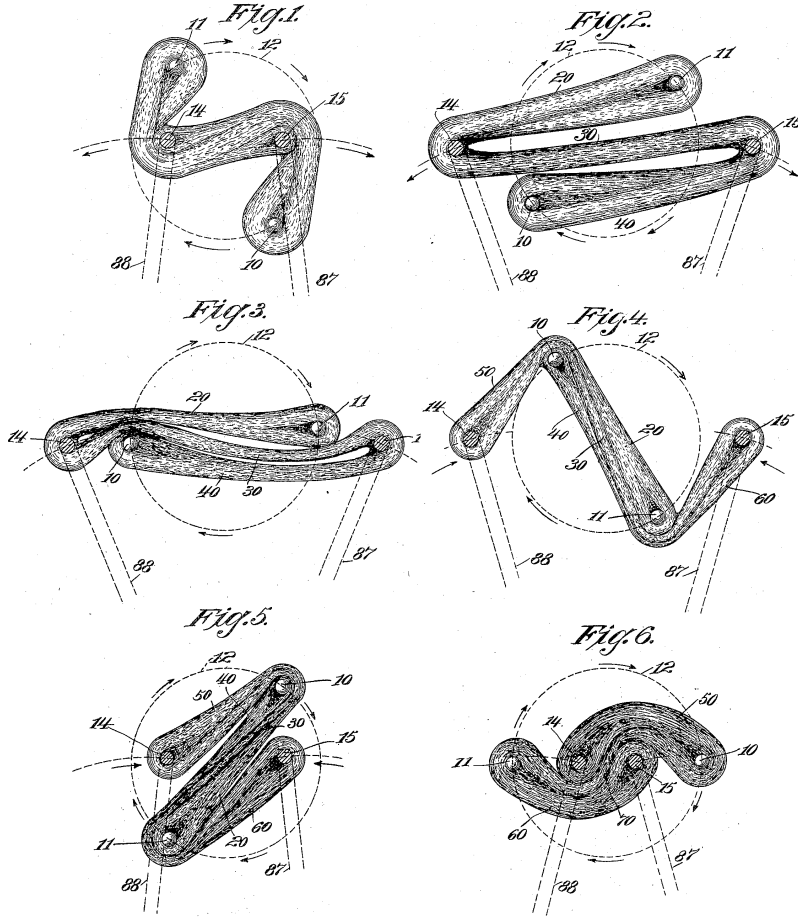


FIGURE 9. Action of the taffy puller patented by Richards (1905). The rod motion is equivalent (conjugate) to that of Fig. 8.

a period-2 point of ϕ will do, as long as the two iterates are also mapped to each other by ι . The map (6) actually has 14 orbits of period 2, but only two of those are also invariant under ι :

$$(8) \quad \left\{ \begin{pmatrix} 1 \\ 4 \\ 0 \end{pmatrix}, \begin{pmatrix} 3 \\ 4 \\ 0 \end{pmatrix} \right\} \quad \text{and} \quad \left\{ \begin{pmatrix} 1 \\ 4 \\ 1 \\ 2 \end{pmatrix}, \begin{pmatrix} 3 \\ 4 \\ 1 \\ 2 \end{pmatrix} \right\}.$$

The second choice would lead to the boundary point being between two rods, so we choose the first orbit. The two iterates are labeled 0_1 and 0_2 in Fig. 10(a). They are interchanged in Fig. 10(b) after applying the map (6), but they both map to the same point on the sphere $S_{0,5} = (T^2/\iota) - \{0\}$, since they also satisfy $\iota(0_1) = 0_2$.

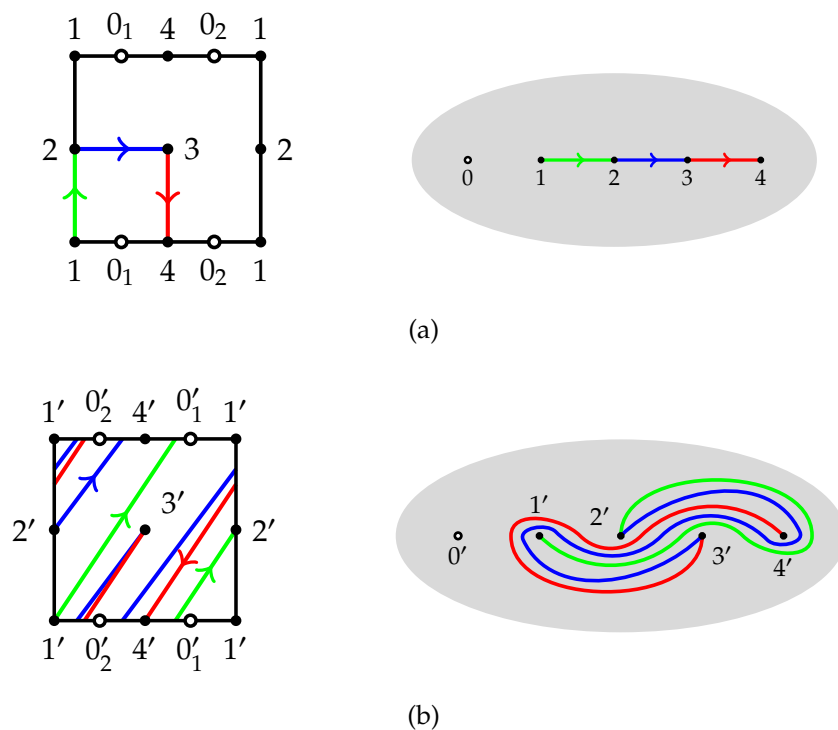


FIGURE 10. (a) Three curves on the torus T^2 (left), which project to curves on the punctured sphere $S_{0,5}$ (right). (b) The three curves transformed by the map (6) (left), and projected onto $S_{0,5}$ (right). Compare these to the last frame of Fig. 9.

Another example of a 4-rod taffy puller arising directly from an Anosov map on the torus is a design of Thibodeau (1904) shown in Fig. 11. It consists of three rods moving in a circle, and a fourth rod crossing their path back and forth. This taffy puller can be shown to come from the same Anosov as gave us the 3-rod puller in Fig. 4, with dilatation equal to the square of the Golden Ratio. Thus, if one is interested in building a device with a Golden Ratio dilatation, the design in Fig. 11(a) is probably far easier to implement than Nitz's in Fig. 4(b), since Thibodeau's does not involve rods being exchanged between two gears.

3.3. A six-rod taffy puller. We mentioned the theorem of Franks and Rykken (1999) at the start of Section 3.2, but so far we have not given an example of a device with a quadratic dilatation that arises from a *branched cover* of the torus, rather than directly from the torus itself. Figure 12 shows such a device, designed and built by Alexander Flanagan and the author. It is a simple modification of the

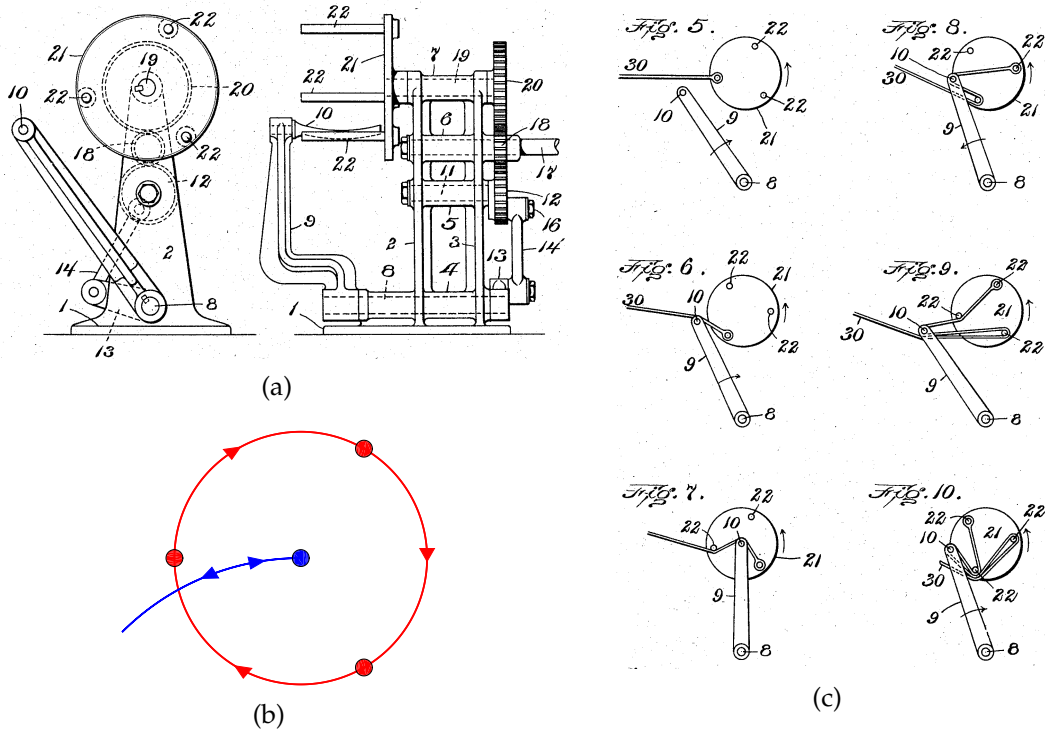


FIGURE 11. (a) Taffy puller from the patent of Thibodeau (1904), with three rotating rods on a wheel and an oscillating arm. (b) Rod motion. (c) The action of the taffy puller, as depicted in the patent.

standard 4-rod design (Fig. 8), except that the two arms of the motion are of equal lengths, and the axles are extended to become fixed rods. There are thus 6 rods in play, and this device has a rather large dilatation.

The construction of this 6-rod device from an Anosov uses the two involutions of the closed (unpunctured) genus two surface S_2 shown in Fig. 13. Imagine that an Anosov map gives the dynamics on the left ‘torus’ of the surface. The involution ι_1 extends those dynamics to a genus two surface by branching at two points. The involution ι_2 is then used to create the quotient surface $S_{0,6} = S_2/\iota_2$. The 6 punctures will correspond to the rods of the taffy puller.

A bit of experimentation suggests starting from the Anosov map

$$(9) \quad \phi(x) = \begin{pmatrix} -1 & -1 \\ -2 & -3 \end{pmatrix} \cdot x.$$

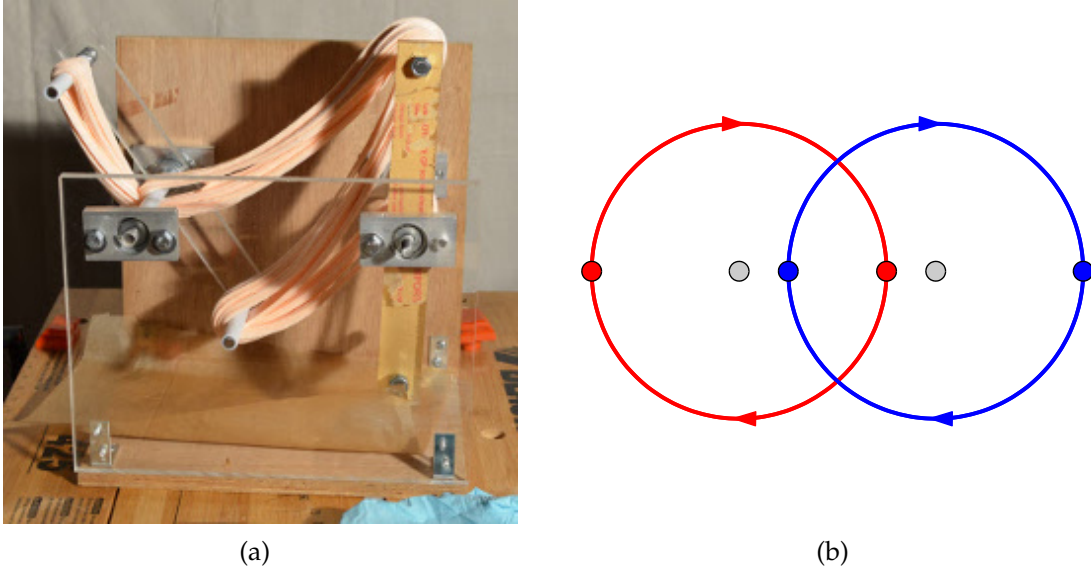


FIGURE 12. (a) A 6-pronged taffy puller designed and built by Alexander Flanagan and the author. (b) The motion of the rods, with two fixed axes.

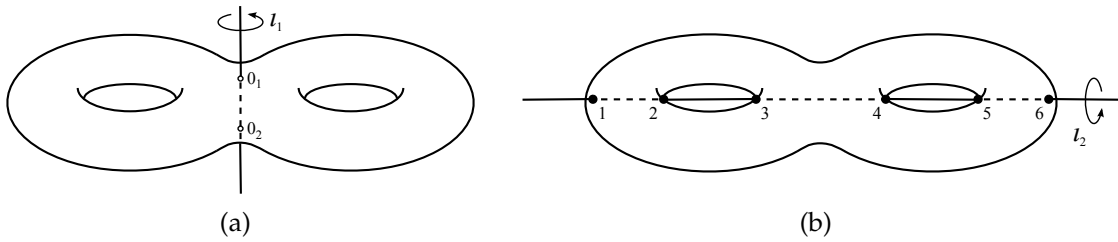


FIGURE 13. The two involutions of a genus two surface S_2 as rotations by π . (a) The involution ι_1 has two fixed points; (b) ι_2 has six.

Referring to the points (1), this map fixes p_0 and p_1 and interchanges p_2 and p_3 . For our purposes, we cut our unit cell for the torus slightly differently, as shown in Fig. 14(a). In addition to p_0 and p_1 , the map has four more fixed points:

$$(10) \quad \begin{pmatrix} -\frac{1}{3} \\ \frac{1}{3} \end{pmatrix}, \begin{pmatrix} \frac{1}{3} \\ \frac{1}{3} \end{pmatrix}, \begin{pmatrix} \frac{1}{6} \\ \frac{2}{3} \end{pmatrix}, \begin{pmatrix} -\frac{1}{6} \\ \frac{1}{3} \end{pmatrix}.$$

To create our branched cover of the torus, we will make a cut from the point $0_1 = (-\frac{1}{3} \ -\frac{1}{3})^T$ to $0_2 = (\frac{1}{3} \ \frac{1}{3})^T$, as shown in Fig. 14(b). We have also labeled by 1–6

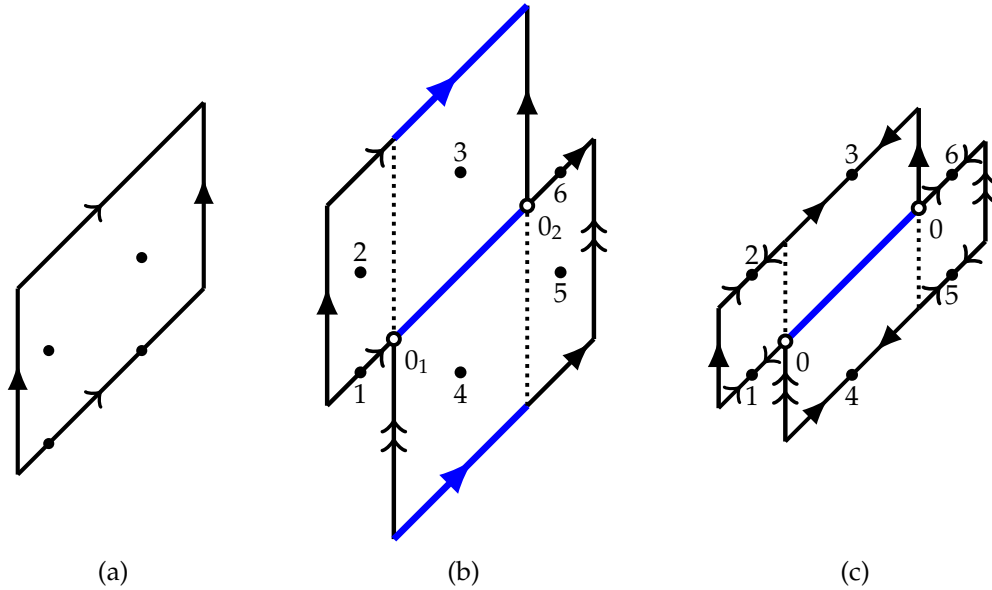


FIGURE 14. (a) A different unfolding of the torus. The four fixed points of ι are indicated. (b) Two copies of the torus glued together after removing a disk. The points $0_{1,2}$ are at $\mp \left(\frac{1}{3}, \frac{1}{3}\right)^T$. This gives the genus two surface S_2 . The two tori are mapped to each other by the involution ι_1 from Fig 13, with fixed points $0_{1,2}$. The involution ι_2 acts on the individual tori with fixed points $1, \dots, 6$. (c) The quotient surface S_2/ι_2 , which is the punctured sphere $S_{0,6}$.

the points that will correspond to our rods. The arrows show identified opposite edges; we have effectively cut a slit in two tori, opened the slits into disks, and glued the tori at those disks to create a genus two surface. The involution ι_1 from Fig. 13(a) corresponds to translating the top half in Fig. 14(b) down to the bottom half; the only fixed points are then 0_1 and 0_2 . For the involution ι_2 of Fig. 13(b), first divide Fig. 14(b) into four sectors with 2–5 at their center; then rotate each sector by π about its center. This fixes the points 1–6. The quotient surface S_2/ι_2 gives the punctured sphere $S_{0,6}$, shown in Fig. 14(c). The points $0_{1,2}$ are mapped to each other by ι_2 and so become identified with the same point 0.

In Fig. 15(a) we reproduce the genus two surface, omitting the edge identifications for simplicity, and draw some arcs between our rods. Now act on the surface (embedded in the plane) with the map (9). The polygon gets stretched, and we must cut and glue pieces following the edge identifications to bring it back into its

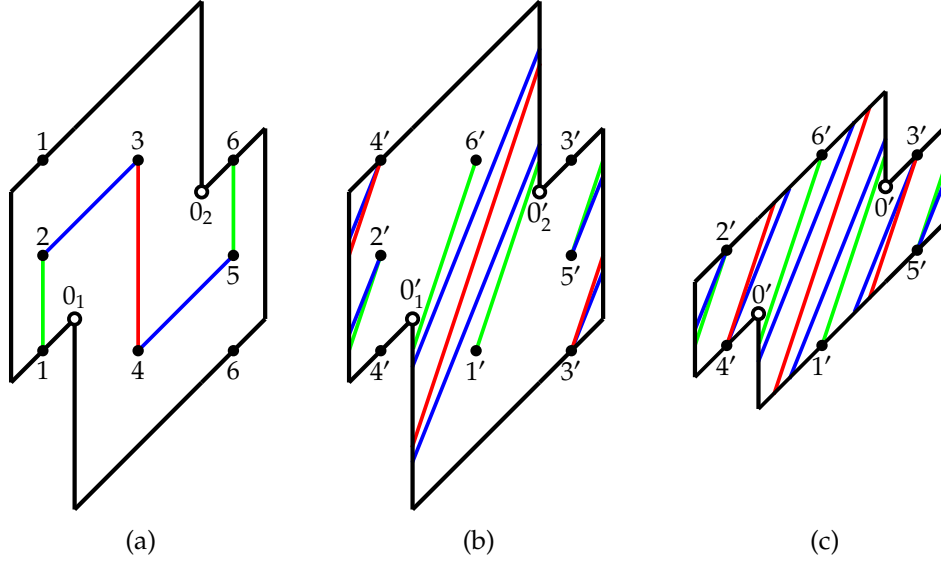


FIGURE 15. (a) The genus two surface from Fig. 14(b), with opposite edges identified and arcs between the rods. (b) The surface and arcs after applying the map (9) and using the edge identifications to cut up and rearrange the surface to the same initial domain. (c) The arcs on the punctured sphere $S_{0,6} = S_2/\iota_2$, with edges identified as in Fig. 14(c).

initial domain, as in Fig. 15(b). Punctures 2 and 5 are fixed, 1 and 4 are swapped, as are 3 and 6. This is exactly the same as for a half-revolution in Fig. 12(b).

After acting with the map we form the quotient surface $S_2/\iota_2 = S_{0,6}$, as in Fig. 15(c). Now we can carefully trace out the path of each arc, and keep track of which side of the arcs the punctures lie. The paths in Fig. 15(c) are identical to the arcs in Fig. 16, and we conclude that the map (9) is the correct description of the six-rod puller. Its dilatation is thus the largest root of $x^2 - 4x + 1$, which is $2 + \sqrt{3}$.

The description of the surface as a polygon in the plane, with edge identifications via translations and rotations, comes from the theory of *flat surfaces* (Zorich 2006). In this viewpoint the surface is given a flat metric, and the corners of the polygon correspond to *conical singularities* with infinite curvature. Here, the two singularities $0_{1,2}$ have cone angle 4π , as can be seen by drawing a small circle around the points and following the edge identifications. The sum of the two singularities is 8π , which equals $2\pi(4g - 4)$ by the Gauss–Bonnet formula, with $g = 2$ the genus.

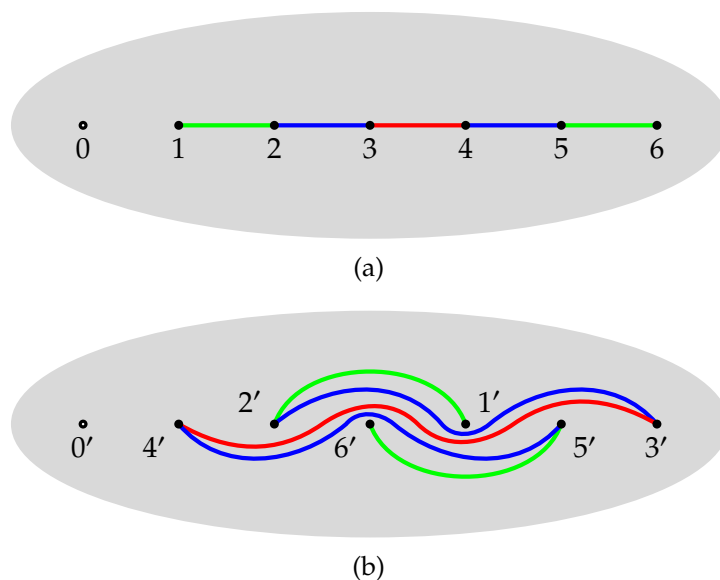


FIGURE 16. (a) A sphere with six punctures (rods) and a seventh puncture at the fixed point 0, with arcs between the punctures, as in Fig. 15(a). (b) The arcs after a half-period of the rod motion in Fig. 12(b). These are identical to the arcs of Fig 15(c).

4. OTHER TYPES OF DEVICES

In the previous section we reviewed several prototypical of taffy pullers, all having a quadratic dilatation. They arise from Anosov maps of the torus, often via some branched covering. In this section we will look at many other designs found in the patent literature. A few of these have a quadratic dilation, but many don't: they involve pseudo-Anosov maps that are more complicated than simple branched covers of the torus. We will not give a detailed construction of the maps, but rather report the polynomial whose largest root is the dilatation and offer some comments. The polynomials were obtained using the computer programs `braidlab` (Thiffeault and Budišić 2013–2016) and `train` (Hall 2012).

4.1. Planetary devices. Planetary devices have rods that move on epicycles, giving their orbits a 'spirograph' appearance. The name comes from Ptolemaic models of the solar system, where planetary motions were apparently well-reproduced using systems of gears. Planetary designs are used in many mixing devices, and are a natural way of creating taffy pullers. Kobayashi and Umeda (2007, 2010) have designed and studied a class of such devices.

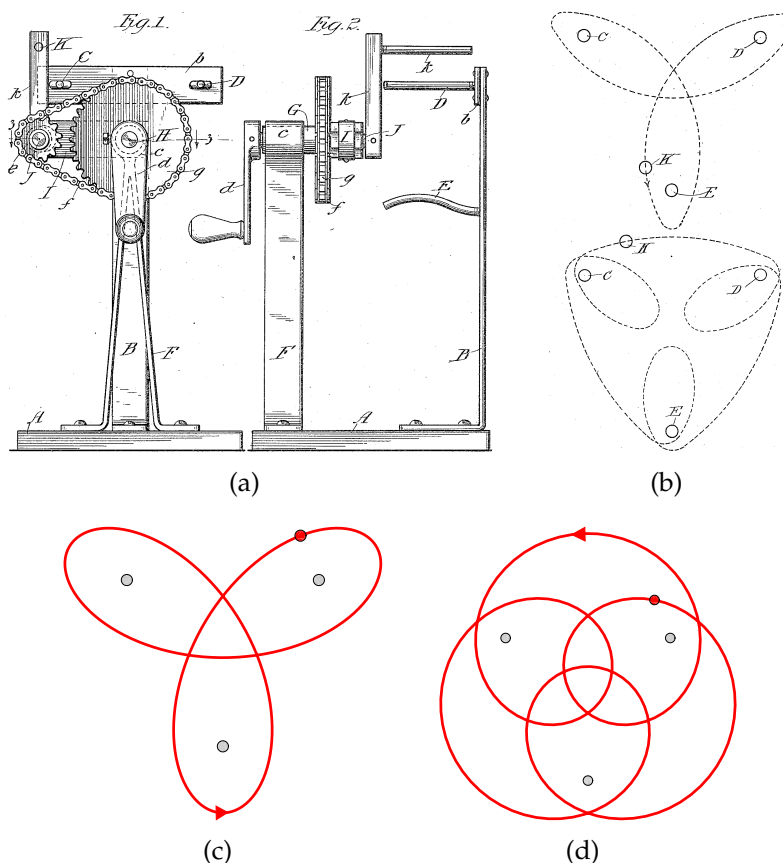


FIGURE 17. (a) Taffy puller from the patent of McCarthy (1916). (b) Rod motion for the two configurations of the device as sketched in the patent. (c) and (d): the actual rod motions.

McCarthy (1916) has an interesting planetary design for a taffy puller (Fig. 17). It has two configurations, with rod motions shown in Fig. 17(b). Its first configuration (pictured in Fig. 17(a) with rod motion as in Fig. 17(c)) is a perfect example of a ' π_1 -stirring device,' a device where only a single rod moves around a set of fixed rods. The optimality of such devices was studied by Boyland and Harrington (2011), and McCarthy's device is one of their optimal examples.

The second configuration (not shown) involves replacing the chain in Fig. 17(a) by two gears in direct contact. This gives the motion in Fig. 17(d), which does appear quite different from McCarthy's sketch (Fig. 17(b), bottom) but is topologically identical. McCarthy himself seemed to prefer the first configuration, as he noted a bit wordily in his patent:

The planetary course described by this pin, when this modified construction is employed, gives a constant pull to the candy, but does not accomplish as thorough mixing of the same as when said pin describes the planetary course resulting from the construction of the preferred form of my invention, as hereinbefore first described.

What he meant by ‘a constant pull to the candy’ is probably that in the second configuration the rod moves back and forth in the center of the device, so the taffy would sometimes be unstretched. In the first configuration the rod resolutely traverses the center of the device in a single direction each time, leading to uniform stretching. As far as the less thorough mixing he mentions is concerned, in one turn of the handle the first configuration gives a dilatation of 4.2361, while the second has 2.4229. However, the second design has a larger dilatation for a full period of the rod motion, as given in Table 1. This illustrates the difficulties involved in comparing the efficiency of different devices, which we will return to in Section 5. In its first configuration the device has a quadratic dilatation, the largest root of $x^2 - 18x + 1$. In its second configuration the dilatation is a quartic number, the largest root of $x^4 - 36x^3 + 5x^2 - 36x + 1$.

Another planetary device, the mixograph, is shown in Fig. 18. The mixograph consists of a small cylindrical vessel with three fixed vertical rods. A lid is lowered onto the base. The lid has two gears each with a pair of rods, and is itself rotating, resulting in a net complex ‘spirograph’ motion as in Fig. 18(c) (top). The mixograph is used to measure properties of bread dough: a piece of dough is placed in the device, and the torque on the rods is recorded on graph paper (in a similar manner to a seismograph). An expert on bread dough can then deduce dough-mixing characteristics from the graph (Connelly and Valenti-Jordan 2008).

Clearly, passing to a uniformly-rotating frame does not modify the dilatation. For the mixograph, a frame where the fixed rods rotate simplifies the orbits somewhat (Fig. 18(c), bottom). This has another advantage: in this ‘co-rotating’ picture, the rods return to their initial configuration (as a set) much sooner than in the fixed picture. This makes the map simpler, and we then take a power of this co-rotating map to recover the original. The rod motion of Fig. 18(c) (bottom) must be repeated *six* times for all the rods to return to their initial position. The dilatation for the co-rotating map is the largest root of $x^8 - 4x^7 - x^6 + 4x^4 - x^2 - 4x + 1$, which is approximately 4.1858.

4.2. A few more designs. The design of Jenner (1905), shown in Fig. 19, is a fairly straightforward variant of the other devices we’ve seen. From our point of view it has a peculiar property: its dilatation is the largest root of the polynomial $x^4 - 8x^3 - 2x^2 - 8x + 1$, which is the strange number $(\varphi + \sqrt{\varphi})^2$, where φ is the Golden Ratio.

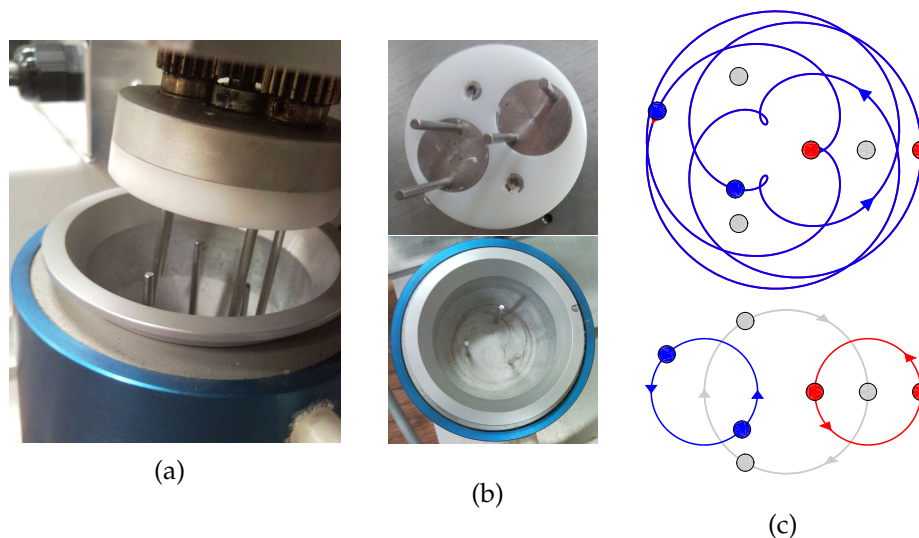


FIGURE 18. (a) The mixograph, a planetary rod mixer for bread dough. (b) Top section with four moving rods (above), and bottom section with three fixed rods (below). (c) The rod motion is complex (top), but is less so in a rotating frame (bottom). (Courtesy of the Department of Food Science, University of Wisconsin. Photo by the author, from Finn and Thiffeault (2011).)

The taffy puller of Shean and Schmelz (1914) is shown in Fig. 20. The design is somewhat novel, since it is not based directly on gears. It consists of two interlocking ‘combs’ of three rods each, for a total of six moving rods. Mathematically, this device has exactly the same dilatation as the earlier 6-rod design (Fig. 12). A similar comb design was later used in a device for homogenizing molten glass (Russell and Wiley 1951).

We finish with the intriguing design of McCarthy and Wilson (1915), shown in Fig. 21. This is the most baroque design we’ve encountered: it contains a reciprocating arm, rotating rods, and fixed rods. The inventors did seem to know what they were doing with this complexity: its dilatation is enormous at approximately 21.2667, the largest root of $x^4 - 20x^3 - 26x^2 - 20x + 1$.

5. DISCUSSION

The reader might be wondering at this point: which is the best taffy puller in history? Did all these incremental changes and new designs lead to measurable progress in the effectiveness of taffy pullers? Table 1 collects the characteristic

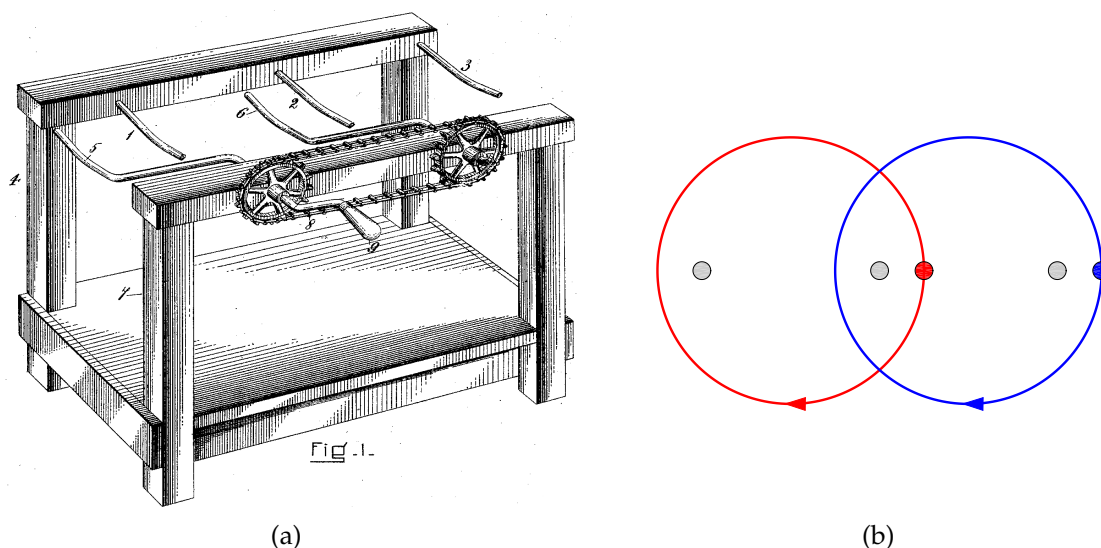


FIGURE 19. Taffy puller from the patent of Jenner (1905). (b) The motion of the rods, with three fixed rods in gray.

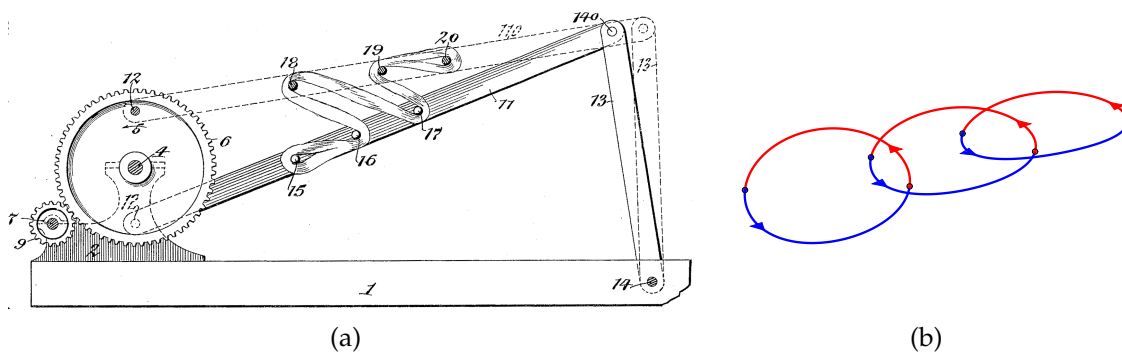


FIGURE 20. (a) Taffy puller from the patent of Shean and Schmelz (1914). (b) The rod motion.

polynomials and the dilatations (the largest root) for all the taffy pullers discussed here. The total number of rods is listed (the number in parentheses is the number of fixed rods).

The column labeled p requires a bit of explanation. Comparing the different taffy pullers is not straightforward. For example, for the first mode of operation of the device by McCarthy (1916), in Fig. 17(c), two full turns of the crank are required for the rod to come back to its initial position. For the second mode, in

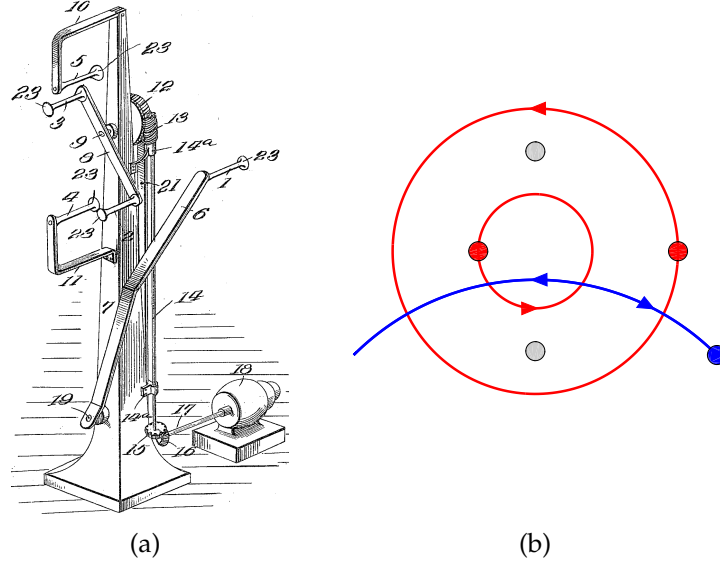


FIGURE 21. (a) Taffy puller from the patent of McCarthy and Wilson (1915). (b) Rod motion.

Fig. 17(d), *four* turns are required. The second mode has a larger dilatation, but it clearly requires more work. A full characterization of the efficiency of a taffy puller would have to take into account the torque required to pull the candy.

To keep things simple, we define the efficiency in terms of the total dilatation for a full period, where a full period is defined by all the rods returning to their initial positions. For example, referring to Table 1, for the Thibodeau 1904 device the rods return to the same configuration as a set after $p = 1/3$ of a period. Hence, the dilatation listed, φ^2 is for $1/3$ of a period. We define its efficiency as the entropy (logarithm of the dilatation) per period. Hence, in this case the efficiency is $\log(\varphi^2)/(1/3) = 6 \log \varphi \approx 2.8873$.

By this measure, the mixograph is the clear winner, with a staggering efficiency of 8.5902. Of course, it also has the most rods. The large efficiency is mostly due to how long the rods take to return to their initial position.

Some observations can be made regarding the taffy pullers presented. With a few exceptions, they all give pseudo-Anosov maps. The inventors were thus aware, at least intuitively, that there should be no unnecessary rods.

Another observation is that most of the dilatations are quadratic numbers. There are probably a few reasons for this. One is that the polynomial giving the dilatation expresses a recurrence relation that characterizes how the folds are combined at each period. With a small number, of rods, there is a limit to the degree of

TABLE 1. Efficiency of taffy pullers. A number of rods such as 6 (2) indicates 6 total rods, with 2 fixed. The largest root of the polynomial is the dilatation. The dilatation corresponds to a fraction p of a full period, when each rod returns to its initial position. The entropy per period is $\log(\text{dilatation})/\text{period}$, which is a crude measure of efficiency. Here $\varphi = \frac{1}{2}(1 + \sqrt{5})$ is the Golden Ratio, and $\chi = 1 + \sqrt{2}$ is the Silver Ratio.

puller	fig.	rods	polynomial	dilatation	p	entropy/ period
standard 3-rod	3	3 (1)	$x^2 - 6x + 1$	χ^2	1	1.7627
Nitz (1918)	4	3	$x^2 - 3x + 1$	φ^2	$1/3$	2.8873
standard 4-rod	8	4	$x^2 - 6x + 1$	χ^2	1	1.7627
Thibodeau (1904)	11	4	$x^2 - 3x + 1$	φ^2	$1/3$	2.8873
6-rod	12	6 (2)	$x^2 - 4x + 1$	$2 + \sqrt{3}$	$1/2$	2.6339
McCarthy (1916) †	17(c)	4 (3)	$x^2 - 18x + 1$	φ^6	1	2.8873
	17(d)	4 (3)	$x^4 - 36x^3 + 5x^2 - 36x + 1$	34.4634	1	3.5399
mixograph ‡	18(c)	7	$x^8 - 4x^7 - x^6 + 4x^4$	4.1858	$1/6$	8.5902
			$-x^2 - 4x + 1$			
Jenner (1905)	19	5 (3)	$x^4 - 8x^3 - 2x^2 - 8x + 1$	$(\varphi + \sqrt{\varphi})^2$	1	2.1226
Shean (1914)	20	6	$x^2 - 4x + 1$	$2 + \sqrt{3}$	$1/2$	2.6339
McCarthy (1915)	21	5 (2)	$x^4 - 20x^3 - 26x^2 - 20x + 1$	21.2667	1	3.0571

† The McCarthy (1916) device has two configurations.

‡ This is the co-rotating version of the mixograph (Fig. 18(c), bottom).

this recurrence ($2n - 4$ for n rods). A second reason is that more rods does not necessarily mean larger dilatation (Finn and Thiffeault 2011). On the contrary, more rods allows for a smaller dilatation, as observed when finding the smallest value of the dilatation (Hironaka and Kin 2006; Lanneau and Thiffeault 2011; Thiffeault and Finn 2006; Venzke 2008).

The collection of taffy pullers presented here can be thought of as a battery of examples to illustrate various types of pseudo-Anosov maps. Even though they did not come out of the mathematical literature, they predate by many decades the examples that were later constructed by many groups (Binder 2010; Binder and Cox 2008; Boyland, Aref, and Stremler 2000; Boyland and Harrington 2011; Finn and Thiffeault 2011; Kobayashi and Umeda 2007, 2010; Thiffeault and Finn 2006).

There are actually quite a few more patents for taffy pullers that were not shown here (only U.S. patents were searched). An obvious question is: why so many? Often the answer is that a new patent is created to get around an earlier one, but the very first patents had lapsed by the 1920s and yet more designs were

introduced, so this is only a partial answer. Perhaps there is a natural response when looking at a taffy puller to think that we can design a better one, since the basic idea is so simple. At least mathematics provides a way of making sure that we've thoroughly explored all designs, and to gauge the effectiveness of existing ones.

REFERENCES

- Binder, B. J. (2010). "Ghost rods adopting the role of withdrawn baffles in batch mixer designs." *Phys. Lett. A* **374**, 3483–3486.
- Binder, B. J. and S. M. Cox (2008). "A mixer design for the pigtail braid." *Fluid Dyn. Res.* **40**, 34–44.
- Boyland, P. L., H. Aref, and M. A. Stremler (2000). "Topological fluid mechanics of stirring." *J. Fluid Mech.* **403**, 277–304.
- Boyland, P. L. and J. Harrington (2011). "The entropy efficiency of point-push mapping classes on the punctured disk." *Algeb. Geom. Topology* **11**(4), 2265–2296.
- Connelly, R. K. and J. Valenti-Jordan (Dec. 2008). "Mixing analysis of a Newtonian fluid in a 3D planetary pin mixer." **86**(12), 1434–1440.
- Dickinson, H. M. (Sept. 1906). "Candy-pulling machine." Pat. US831501 A.
- Farb, B. and D. Margalit (2011). *A Primer on Mapping Class Groups*. Princeton, NJ: Princeton University Press.
- Fathi, A., F. Laudenbach, and V. Poénaru (1979). "Travaux de Thurston sur les surfaces." *Astérisque* **66-67**, 1–284.
- Finn, M. D. and J.-L. Thiffeault (Dec. 2011). "Topological optimization of rod-stirring devices." *SIAM Rev.* **53**(4), 723–743.
- Firchau, P. J. G. (Dec. 1893). "Machine for working candy." Pat. US511011 A.
- Franks, J. and E. Rykken (1999). "Pseudo-Anosov homeomorphisms with quadratic expansion." *Proc. Amer. Math. Soc.* **127**, 2183–2192.
- Halbert, J. T. and J. A. Yorke (2014). "Modeling a chaotic machine's dynamics as a linear map on a "square sphere"." *Topology Proceedings* **44**, 257–284.
- Hall, T. (2012). *Train: A C++ program for computing train tracks of surface homeomorphisms*. http://www.liv.ac.uk/~tobyhall/T_Hall.html.
- Hironaka, E. and E. Kin (2006). "A family of pseudo-Anosov braids with small dilatation." *Algebraic & Geometric Topology* **6**, 699–738.
- Hudson, W. T. (Feb. 1904). "Candy-working machine." Pat. US752226 A.
- Jenner, E. J. (Nov. 1905). "Candy-pulling machine." Pat. US804726 A.
- Kirsch, E. (Jan. 1928). "Candy-pulling machine." Pat. US1656005 A.

- Kobayashi, T. and S. Umeda (2007). "Realizing pseudo-Anosov egg beaters with simple mechanisms." In: *Proceedings of the International Workshop on Knot Theory for Scientific Objects, Osaka, Japan*. Osaka, Japan: Osaka Municipal Universities Press, pp. 97–109.
- (2010). "A design for pseudo-Anosov braids using hypotrochoid curves." *Topology Appl.* **157**, 280–289.
- Lanneau, E. and J.-L. Thiffeault (June 2011). "On the minimum dilatation of braids on the punctured disc." *Geometriae Dedicata* **152**(1), 165–182.
- MacKay, R. S. (2001). "Complicated dynamics from simple topological hypotheses." *Phil. Trans. R. Soc. Lond. A* **359**, 1479–1496.
- McCarthy, E. F. (May 1916). "Candy-pulling machine." Pat. US1182394 A.
- McCarthy, E. F. and E. W. Wilson (May 1915). "Candy-pulling machine." Pat. US1139786 A.
- Nitz, C. G. W. (Sept. 1918). "Candy-puller." Pat. US1278197 A.
- Richards, F. H. (May 1905). "Process of making candy." Pat. US790920 A.
- Robinson, E. M. and J. H. Deiter (Mar. 1908). "Candy-pulling machine." Pat. US881442 A.
- Russell, R. G. and R. B. Wiley (Dec. 1951). "Apparatus for mixing viscous liquids." Pat. US2577920 A.
- Shean, G. C. C. and L. Schmelz (Oct. 1914). "Candy-pulling machine." Pat. US1112569 A.
- Thibodeau, C. (Aug. 1903). "Method of pulling candy." Pat. US736313 A.
- (Oct. 1904). "Candy-pulling machine." Pat. US772442 A.
- Thiffeault, J.-L. and M. D. Finn (Dec. 2006). "Topology, braids, and mixing in fluids." *Phil. Trans. R. Soc. Lond. A* **364**, 3251–3266.
- Thiffeault, J.-L. and M. Budišić (2013–2016). *Braidlab: A Software Package for Braids and Loops*. <http://arXiv.org/abs/1410.0849>, Version 3.2.
- Thurston, W. P. (1988). "On the geometry and dynamics of diffeomorphisms of surfaces." *Bull. Am. Math. Soc.* **19**, 417–431.
- Venzke, R. W. (2008). *Braid Forcing, Hyperbolic Geometry, and Pseudo-Anosov Sequences of Low Entropy*. PhD thesis. California Institute of Technology.
- Zorich, A. (2006). "Flat surfaces." In: *Frontiers in Number Theory, Physics, and Geometry*. Ed. by P. Cartier et al. Vol. 1. Berlin: Springer, pp. 439–586.

DEPARTMENT OF MATHEMATICS, UNIVERSITY OF WISCONSIN, MADISON, WI 53706, USA
 E-mail address: jeanluc@math.wisc.edu